Article

Squeezing Light via Levitated Cavity Optomechanics

Guoyao Li [1] and **Zhang-Qi Yin** [1,2,*]

1   Key Laboratory of Advanced Optoelectronic Quantum Architecture and Measurements (MOE),
    Center for Quantum Technology Research, School of Physics, Beijing Institute of Technology,
    Beijing 100081, China; 3120205731@bit.edu.cn
2   Beijing Academy of Quantum Information Sciences, Beijing 100193, China
*   Correspondence: zqyin@bit.edu.cn

Abstract: Squeezing light is a critical resource in both fundamental physics and precision measurement. Squeezing light has been generated through optical-parametric amplification inside an optical resonator. However, preparing the squeezing light in an optomechanical system is still a challenge for the thermal noise inevitably coupled to the system. We consider an optically levitated nano-particle in a bichromatic cavity, in which two cavity modes could be excited by the scattering photons of the dual tweezers, respectively. Based on the coherent scattering mechanism, the ultra-strong coupling between the cavity field and the torsional motion of nano-particle could be achieved for the current experimental conditions. With the back-action of the optically levitated nano-particle, the broad single-mode squeezing light can be realized in the bad cavity regime. Even at room temperature, the single-mode light can be squeezed for more than 17 dB, which is far beyond the 3 dB limit. The two-mode squeezing light can also be generated, if the optical tweezers contain two frequencies, one is on the red sideband of the cavity mode, the other is on the blue sideband. The two-mode squeezing can be maximized near the boundary of the system stable regime and is sensitive to both the cavity decay rate and the power of the optical tweezers.

Keywords: squeezing light; coherent scattering; levitated optomechanics

1. Introduction

Squeezing light, in which the quantum fluctuation is modulated below the shot noise level, has been regarded as a powerful resource in fundamental physics, e.g., improving the sensitivity of gravitational wave detection [1], cooling the motion of a macroscopic mechanical object below the quantum backaction limit [2], engineering matter interactions [3], and inducing the topological phase transitions [4], among many others. Squeezing light can be generated via the nonlinear optics, such as parametric down-conversion process [5–8]. The motion of the mechanical oscillator in cavity optomechanical systems could be regarded as an effective nonlinear optical medium, generating the pondermotive squeezing state by the back-action interaction [8–11]. With various optomechanical coupling mechanisms, cavity optomechanical systems produce abundant squeezing light sources [11–15], even in pulse driving regime [11,15]. However, due to the noise inevitably induced from the thermal bath, as well as the limitation of the nonlinear interaction, generating the substantial pondermotive squeezing light is still a challenge for the optomechanical system [9].

The levitated optomechanical system has raised widespread interest in macroscopic quantum superposition [16–18], quantum time crystals [19,20], and quantum information processing [21]. The squeezing has been studied in the levitated optomechanical system, in which the nano-particle is optically levitated and coupled with a cavity field [22]. Under ultra-high vacuum (gas pressure $p = 10^{-10}$ Torr), the squeezing light could be estimated over 15 dB below the vacuum noise level [22], which is much higher than the squeezing light source based on a membrane mechanical resonator embedded in an optical cavity [9].

In the levitated optomechanical system, the motional state of the optically levitated nano-particle has been squeezed 2.7 dB below the thermal noise [23]. Recently, the coherent scattering mechanism has been theoretically investigated to cool both the axial and the in-plane motion of the levitated optomechanical system via a cavity mode [24,25]. The axial motion of the optically levitated nano-particle has been cooled to the ground state, either through the coherent scattering induced cavity cooling [26,27], or through the feedback cooling [28,29]. Moreover, the strong coherent scattering coupling between the cavity field and the motion of the nano-particle has also been observed in experiment [30]. With the attainable ultra-high quality factor (beyond 10^9) of the optically nano-particle [31–33], it is expected that the stronger and robust squeezing light can be realized via the coherent scattering [22,24,32,34,35].

In this paper, we aim to generate both single-mode and two-mode squeezing light via a vacuum levitated optomechanical system, in which the nano-particle is optically levitated by the single and dual tweezers, respectively [22,24]. Both schemes are based on the coherent scattering mechanism [24]. We find that the ultra-strong coupling between the cavity mode and the torsion mode of the nano-particle is available by the current experimental parameters [36–39]. In order to obtain the squeezed single-mode light in steady state, the optical tweezers are detuned to the red sideband of the cavity mode. By the back-action of the optically levitated nano-particle [11], the single-mode light can be squeezed over 17 dB. The strong and broad single-mode squeezing light is observed in a bad cavity. Furthermore, in order to generate the two-mode squeezing lightly, we consider the optical tweezers with two frequencies, one is on the red sideband of the cavity mode, the other is on the blue sideband. We find that the two-mode squeezing can be maximized when the dynamics approach system instability [40]. The squeezing is sensitive to both the cavity decay rate and optical tweezers' power. Unlike the single-mode squeezing light, the generated two-mode squeezing light is also an entangling source, which is very sensitive to thermal noise. We also find that the two-mode squeezing degree is smaller than the single-mode squeezing.

The paper is organized as follows. The model and the system dynamics are depicted in Section 2. Then the results of one-mode squeezing light and two-mode squeezing light are discussed in Sections 3 and 4. At last, a brief conclusion is given in Section 5.

2. Model and Dynamics

We consider a uniform isotropic non-dispersive nano-ellipsoid, which is optically levitated by linearly polarized dual tweezers (A and B) in a bichromatic cavity as shown in Figure 1a. The optical tweezers A (B) with frequency $\omega_{A(B)}$ are on the red (blue) sideband of cavity mode $\hat{a}_A$ ($\hat{a}_B$). Under this condition, the nano-ellipsoid will be cooled and heated by the optical tweezers A and B, respectively. If the cooling rate is larger than the heating rate, the motional state can be cooled down to a low temperature and the system remains dynamically stable.

The motion of the levitated nano-ellipsoid is characterized by the five degrees of freedom where $\{x, y, x\}$ for the center-of-mass motion in position $\hat{R}$ and $\{\theta, \phi\}$ for the torsional motion in orientation $\hat{\Omega}$, as shown in Figure 1b. By locating the nano-ellipsoid to the node (anti-node) of the cavity modes, the center-of-mass motion and torsional motion can be decoupled from each other [37]. Besides, intrinsic optomechanical coupling between the cavity mode and torsional motion of the nano-ellipsoid is typically much weaker than the coherent scattering coupling strength [24,26,37]. Therefore, we only consider the coherent scattering coupling between the cavity mode and the motion of the nano-ellipsoid. Without loss of generality, we take the torsional motion as an example in the following discussion [38,39].
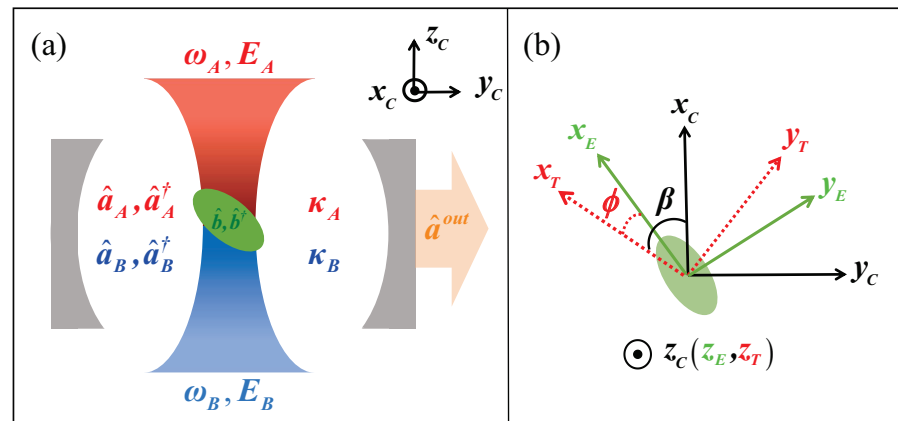
Figure 1. (**a**) Schematic diagram of the levitated optomechanical system. The nano-ellipsoid is placed into a bichromatic cavity and optically levitated by the dual tweezers with two frequencies ω_A and ω_B, and amplitudes E_A and E_B, respectively. Two cavity modes $\hat{a}_A^\dagger$ ($\hat{a}_A$) and $\hat{a}_B^\dagger$ ($\hat{a}_B$) are excited by the scattering photons with the decay rates κ_A and κ_B. (**b**) The orientation of the nano-ellipsoid $\{x_E, y_E, z_E\}$ rotates under the tweezers coordinate $\{x_T, y_T, z_T\}$ with a small angel ϕ. β is the angel between the cavity coordinate axis x_C and tweezers coordinate axis x_T. Tweezers propagate along the direction of axis z_T.

With respect to the interaction picture defined by the Hamiltonian $H_0 = \hbar \sum\limits_{j=A,B} \omega_j a_j^\dagger a_j$, the interaction Hamiltonian for the system can be written as [24]

$$\hat{H} = \hbar \sum_{j=A,B} \Delta_j \hat{a}_j^\dagger \hat{a}_j + \hbar \omega_m \hat{b}^\dagger \hat{b} - \hbar \sum_{j=A,B} g_j \left(\hat{a}_j^\dagger + \hat{a}_j\right)\left(\hat{b}^\dagger + \hat{b}\right), \tag{1}$$

where $\hat{a}_j^\dagger$ and $\hat{a}_j$ ($\hat{b}^\dagger$ and $\hat{b}$) are the bosonic creation and annihilation operators with the commutation relations $\left[\hat{a}_j, \hat{a}_j^\dagger\right] = 1$ ($\left[\hat{b}, \hat{b}^\dagger\right] = 1$) [41], $\Delta_j = \omega_c^j - \omega_j$ is the detuning between the cavity frequency ω_c^j and the optical tweezers frequency ω_j. ω_m is the torsional mode frequency and g_j is the coherent scattering coupling. They can be calculated by (see Appendix B)

$$g_j = (\alpha_a - \alpha_b)E_0^j \xi_0 \cos(\varphi) \sqrt{\frac{\omega_c^j}{8\hbar \varepsilon_0 V_c^j}} \tag{2}$$

and

$$\omega_m = \sqrt{\sum_{j=A,B} E_0^{j2}(\alpha_a - \alpha_b) \Big/ 2I} \tag{3}$$

respectively. For the current experimental parameters, the torsional frequency can be in the order of MHz as shown in Figure 2a. Interestingly, the ratio (g_j/ω_m) between the coherent scattering coupling and the torsional frequency is larger than 0.1 as shown in Figure 2b, in which the ultra-strong optomechanical coupling regime has been reached [36]. In this regime, both the rotating and anti-rotating wave terms have to be considered. As $\hat{a}_j$ ($\hat{a}_j^\dagger$) depends on $\hat{b} + \hat{b}^\dagger$, one field quadrature of the cavity mode will be squeezed, while another will be anti-squeezed [5,6].
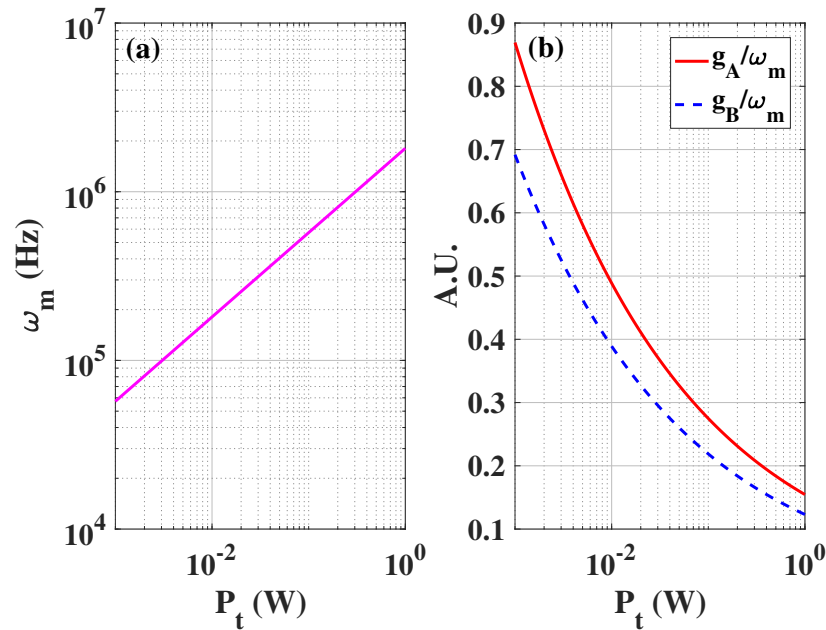
Figure 2. The torsional frequency ω_m (**a**) and the ratio between the coherent scattering coupling and torsional frequency (**b**) as a function of the tweezers power P_t. The parameters are given as follows: the cavity length $L = 1$ mm, the wavelength of the optical tweezers $\lambda_A = 780$ nm ($\lambda_B = 980$ nm), the beam waist of the tweezers in focus $w_0^j = 1$ μm, the principle axes of the nano-ellipsoid $a = 2b = 2c = 100$ nm, the relative permittivity of the nano-ellipsoid $\varepsilon = 2.1$, and the density of the nano-ellipsoid $\rho = 2200$ kg/m^3. For convenience, the power of two optical tweezers are assumed to be the same $P_j = P_t$.

Derived from the system Hamiltonian (1), the dynamics of the system is characterized by the following quantum Langevin equations:

$$\frac{d\hat{b}}{dt} = -\left(\frac{\gamma_m}{2} + i\omega_m\right)\hat{b} + i\sum_{j=A,B} g_j\left(\hat{a}_j^\dagger + \hat{a}_j\right) + \sqrt{\gamma_m}\hat{b}^{in}, \tag{4}$$

$$\frac{d\hat{a}_j}{dt} = -\left(\frac{\kappa_j}{2} + i\Delta_j\right)\hat{a}_j + ig_j\left(\hat{b}^\dagger + \hat{b}\right) + \sqrt{\kappa_j}\hat{a}_j^{in}, \tag{5}$$

where γ_m is the damping rate of the torsional mode (see Appendix C). Note that the operators are already replaced by $\delta\hat{O} \rightarrow \hat{O}$, where $\delta\hat{O}$ denotes the fluctuation of $\hat{O} = \{\hat{a}_j, \hat{b}\}$. $\hat{a}_j^{in}$ and $\hat{b}^{in}$ are the zero-mean Gaussian noises, satisfying the correlation relations $\left\langle \hat{a}_j^{in}(t)\hat{a}_j^{in\dagger}(t')\right\rangle = \delta(t-t')$ and $\left\langle \hat{b}^{in}(t)\hat{b}^{in\dagger}(t')\right\rangle = (\bar{n}+1)\delta(t-t')$ respectively [41]. Here $\bar{n} = \{\exp(\hbar\omega_m/k_BT) -1\}^{-1}$ is the mean thermal excitation numbers at bath temperature T, and k_B is Boltzmann constant. The linearized Langevin Equations (4) and (5) can be rewritten in the matrix form

$$\dot{\hat{f}}(t) = A\hat{f}(t) + \hat{D}(t) \tag{6}$$

where $\hat{f}^T(t) = \{\hat{b}(t), \hat{b}^\dagger(t), \hat{a}_A(t), \hat{a}_A^\dagger(t), \hat{a}_B(t), \hat{a}_B^\dagger(t)\}$ and $\hat{D}^T(t) = \{\sqrt{\gamma_m}\hat{b}^{in}(t), \sqrt{\gamma_m}\hat{b}^{in\dagger}(t), \sqrt{\kappa_A}\hat{a}_A^{in}(t), \sqrt{\kappa_A}\hat{a}_A^{in\dagger}(t), \sqrt{\kappa_B}\hat{a}_B^{in}(t), \sqrt{\kappa_B}\hat{a}_B^{in\dagger}(t)\}$. The drift matrix A is given by

$$A = \begin{pmatrix} -\frac{\gamma}{2} - i\omega_m & 0 & ig_A & ig_A & ig_B & ig_B \\ 0 & -\frac{\gamma}{2} + i\omega_m & -ig_A & -ig_A & -ig_B & -ig_B \\ ig_A & ig_A & -\frac{\kappa_A}{2} - i\Delta_A & 0 & 0 & 0 \\ -ig_A & -ig_A & 0 & -\frac{\kappa_A}{2} + i\Delta_A & 0 & 0 \\ ig_B & ig_B & 0 & 0 & -\frac{\kappa_B}{2} - i\Delta_B & 0 \\ -ig_B & -ig_B & 0 & 0 & 0 & -\frac{\kappa_B}{2} + i\Delta_B \end{pmatrix}. \tag{7}$$

After the Fourier transform $\hat{O}(t) = \int_{-\infty}^{+\infty} \hat{O}(\omega) e^{-i\omega t} d\omega$, the steady state solutions of the Langevin Equations (4) and (5) in the frequency domain are

$$\hat{b}(\omega) = \frac{i \sum_{j=A,B} g_j \left[\hat{a}_j^\dagger(-\omega) + \hat{a}_j(\omega) \right] + \sqrt{\gamma_m} \hat{b}^{in}}{\frac{\gamma_m}{2} + i(\omega_m - \omega)}, \tag{8}$$

$$\hat{a}_j(\omega) = \frac{ig_j \left(\hat{b}^\dagger(-\omega) + \hat{b}(\omega) \right) + \sqrt{\kappa_j} \hat{a}_j^{in}}{\frac{\kappa_j}{2} + i(\Delta_j - \omega)}, \tag{9}$$

where the corresponding correlation noises are $\left\langle \hat{b}^{in}(\omega) \hat{b}^{in\dagger}(-\omega') \right\rangle = 2\pi(2\bar{n} + 1)\delta(\omega + \omega')$ and $\left\langle \hat{a}_j^{in}(\omega) \hat{a}_{j'}^{in\dagger}(-\omega') \right\rangle = 2\pi\delta_{jj'}(\omega + \omega')$, respectively. Furthermore, Equations (8) and (9) can be rewritten as $\hat{A}(\omega) = J^{-1}(\omega)\hat{B}(\omega)$ where $\hat{A}(\omega) = \{\hat{b}(\omega), \hat{b}^\dagger(-\omega), \hat{a}_A(\omega), \hat{a}_A^\dagger(-\omega),$ $\hat{a}_B(\omega), \hat{a}_B^\dagger(-\omega)\}^T$, $B(\omega) = \{\sqrt{\gamma_m}\hat{b}^{in}(\omega), \sqrt{\gamma_m}\hat{b}^{in\dagger}(-\omega), \sqrt{\kappa_A}\hat{a}_A^{in}(\omega), \sqrt{\kappa_A}\hat{a}_A^{in\dagger}(-\omega),$ $\sqrt{\kappa_B}\hat{a}_B^{in}(\omega), \sqrt{\kappa_B}\hat{a}_B^{in\dagger}(-\omega)\}^T$,

$$J(\omega) = \begin{bmatrix} u_1 & 0 & -ig_A & -ig_A & -ig_B & -ig_B \\ 0 & u_2 & ig_A & ig_A & ig_B & ig_B \\ -ig_A & -ig_A & v_1 & 0 & 0 & 0 \\ ig_A & ig_A & 0 & v_2 & 0 & 0 \\ -ig_B & -ig_B & 0 & 0 & w_1 & 0 \\ ig_B & ig_B & 0 & 0 & 0 & w_2 \end{bmatrix}, \tag{10}$$

$u_1 = \frac{\gamma_m}{2} + i(\omega_m - \omega)$, $u_2 = \frac{\gamma_m}{2} - i(\omega_m + \omega)$, $v_1 = \frac{\kappa_A}{2} + i(\Delta_A - \omega)$, $v_2 = \frac{\kappa_A}{2} - i(\Delta_A + \omega)$, $w_1 = \frac{\kappa_B}{2} + i(\Delta_B - \omega)$, and $w_2 = \frac{\kappa_B}{2} + i(\Delta_B - \omega)$. Based on the standard input–output relation

$$\hat{a}_j^{out}(\omega) = \sqrt{\kappa_j}\hat{a}_j(\omega) - \hat{a}_j^{in}(\omega), \tag{11}$$

the output cavity mode $a_j^{out}(\omega)$ can be attainable.

3. Single-Mode Squeezing

We consider the case that the nano-ellipsoid is levitated by only one optical tweezer A, while the other optical tweezer B is turned off. Only one cavity mode $\hat{a}_A$ is excited by the scattering photons of the optical tweezers A. From Equations (8) and (9), the cavity mode $\hat{a}_A(\omega)$ can be solved as

$$\hat{a}_A(\omega) = m_1^A(\omega)\hat{b}^{in}(\omega) + m_2^A(\omega)\hat{b}^{in\dagger}(-\omega) + m_3^A(\omega)\hat{a}_A^{in}(\omega) + m_4^A(\omega)\hat{a}_A^{in\dagger}(-\omega) \tag{12}$$

where

$$m_1^A(\omega) = i\sqrt{\gamma_m}g_A u_2 v_2/z,$$

$$m_2^A(\omega) = i\sqrt{\gamma_m}g_A u_1 v_2/z,$$

(13)

$$m_3^A(\omega) = \sqrt{\kappa_A}\{g_A^2(u_1 - u_2) + u_1 u_2 v_2\}/z,$$

$$m_4^A(\omega) = \sqrt{\kappa_A}g_A^2(u_1 - u_2)/z,$$

with $z = g_A^2(u_1 - u_2)(v_1 - v_2) + u_1 u_2 v_1 v_2$. Furthermore, substituting Equation (12) in Equation (11), one can obtain the stationary squeezing spectrum of the transmitted field [6]:

$$S_\vartheta(\omega) = \langle \delta X_\vartheta^{out}(\omega)\delta X_\vartheta^{out}(\omega')\rangle$$

(14)

where $\delta X_\vartheta^{out}(\omega) = e^{-i\vartheta}a_A^{out}(\omega) + e^{i\vartheta}a_A^{out\dagger}(-\omega)$ with ϑ being the measurement phase angle in homodyne detection. Or more specifically, Equation (14) can be rewritten as the form of $S_\vartheta(\omega) = S_{\hat{a}\hat{a}^\dagger} + S_{\hat{a}^\dagger\hat{a}} + [e^{-2i\vartheta}S_{\hat{a}\hat{a}} + c.c]$ where

$$\begin{aligned}S_{\hat{a}\hat{a}^\dagger}(\omega) =& \left\langle \hat{a}_A^{out}(\omega)\hat{a}_A^{out\dagger}(-\omega')\right\rangle \\ =& \kappa_A\left[m_3^A(\omega) - 1/\sqrt{\kappa_A}\right]\left[m_3^{A*}(\omega) - 1/\sqrt{\kappa_A}\right] \\ &+ \kappa_A\left[(\bar{n}+1)m_1^A(\omega)m_1^{A*}(\omega) + \bar{n}m_2^A(\omega)m_2^{A*}(\omega)\right],\end{aligned}$$

(15)

$$\begin{aligned}S_{\hat{a}^\dagger\hat{a}}(\omega) =& \left\langle \hat{a}_A^{out\dagger}(-\omega)\hat{a}_A^{out}(\omega')\right\rangle \\ =& \kappa_A\left[\left|m_4^A(-\omega)\right|^2 + (\bar{n}+1)\left|m_2^A(-\omega)\right|^2 + \bar{n}\left|m_1^A(-\omega)\right|^2\right],\end{aligned}$$

(16)

and

$$\begin{aligned}S_{\hat{a}\hat{a}}(\omega) =& \langle \hat{a}_A^{out}(\omega)\hat{a}_A^{out}(\omega')\rangle \\ =& \kappa_A\left[m_3^A(\omega) - 1/\sqrt{\kappa_A}\right]m_4^A(-\omega) \\ &+ \kappa_A\left[(\bar{n}+1)m_1^A(\omega)m_2^A(-\omega) + \bar{n}m_2^A(\omega)m_1^A(-\omega)\right].\end{aligned}$$

(17)

It is noted that the maximum squeezing could reach when $dS_\vartheta(\omega)/\vartheta = 0$. Then it is easy to find out that the maximum squeezing of single output cavity mode is [13,42]

$$S_1(\omega) = S_{\hat{a}\hat{a}^\dagger}(\omega) + S_{\hat{a}^\dagger\hat{a}}(\omega) - 2|S_{\hat{a}\hat{a}}(\omega)|$$

(18)

as $e^{2i\vartheta} = -S_{\hat{a}\hat{a}}/|S_{\hat{a}\hat{a}}|$. The output cavity mode is squeezed if $S_1(\omega)$ decreases below the shot-noise level ($S_1(\omega) < 1$).

In order to maintain the system stability, we assume that the frequency of the optical tweezer A is on the red sideband of the cavity mode, e.g. $\Delta_A = \omega_m$. We find that the Routh–Hurwitz criterion could be fulfilled, even under ultra-strong coupling regime $g_A/\omega_m > 0.1$ [41]. Besides, the cavity mode could be highly squeezed in this regime. As shown in Figure 3, we find that the output cavity mode can be squeezed even at room temperature. Obviously, the optimal squeezing of the output cavity field occurs around resonance regime $\omega = 0$, where the dissipative part of the mechanical susceptibility has no response in dynamics [6]. In the good cavity regime $\kappa_A < \omega_m$, the pondermotive squeezing will be suppressed [15]. As the cavity decay rate increases from $\kappa_A = 0.1\omega_m$ to $\kappa_A = 1\omega_m$, the minimum of $S_1(\omega)$ decreases. The output cavity mode can be squeezed up to 17 dB when the lifetime of cavity photons approximately equals to a period of torsional motion ($\kappa_A \approx \omega_m$). As the cavity decay rate continues to increase, the broadband and strong squeezing generate a bad cavity condition $\kappa_A \approx 2\omega_m$. Then the broadband squeezing will split into two dips under the bad cavity regime, and the squeezing degree will reduce at $\omega = 0$ for the larger dissipation [15].

Note that the model we proposed is an open system, in which the optically levitated nano-ellipsoid irreversibly couples to the environment by the collision of the surrounding gas [33]. With the back-action interaction, the thermal disturbance could act on cavity mode, leading to decoherence. Here we investigate the effects on the squeezing light from the perspective of the surrounding gas pressure and temperature of the torsional motion. As shown in Figure 4a, $S_1(\omega)$, this depends on the gas pressure p. The lower pressure of the surrounding gas leads to the higher squeezing light. However, limited by the stability in ultra-high vacuum and the photons recoiling [33], the squeezing threshold exists. On the other hand, the higher temperature for the torsional mode will extremely enlarge the number of thermal phonons, which would destroy the squeezing state of the output lights. Therefore, many schemes based on optomechanics require a low-temperature environment [9,11,23]. In order to realize the stronger squeezing light, the high-quality factor and low-temperature environment are necessary for the levitated optomechanical system [11]. For our scheme, the squeezing is robust to the thermal environment as shown in Figure 4b.
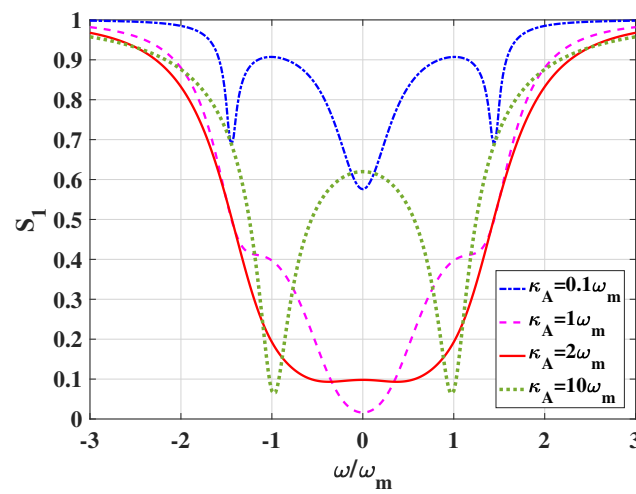

Figure 3. $S_1(\omega)$ as a function of the cavity decay rate κ_A. Parameters are listed as follows: optical tweezers' power in focus $P_A = 0.05$ W, pressure of the residual gas $p = 10^{-4}$ Pa, temperature of the residual gas $T_a = 300$ K, bath temperature for the torsional mode $T = 300$ K, and the accommodation efficient $\gamma_{ac} = 0.9$ (see Appendix C). Other parameters are the same as Figure 2.
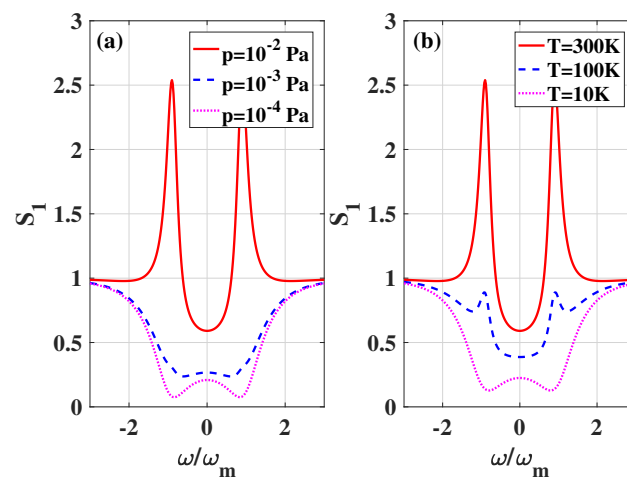

Figure 4. $S_1(\omega)$ as a function of the pressure of the surrounding gas p (**a**) and the temperature of torsional mode T (**b**). In pictures (**a**), the temperature of the torsional mode is assumed $T = 300$ K, while the pressure of residual gas is set to 10^{-2} Pa in picture (**b**). The cavity decay rate is $\kappa_A = 3\omega_m$ in both picture (**a**,**b**). Other parameters are the same as Figure 3.

4. Two-Mode Squeezing

Our scheme can also be used for generating two-mode squeezing light, if we consider the nano-ellipsoid is optically levitated by dual tweezers, both A and B. Driven by the scattering photons, two cavity modes $\hat{a}_A$ and $\hat{a}_B$ are excited in the bichromatic cavity. Based on Equations (8), (9), and (11), the output cavity mode $\hat{a}_j^{out}(\omega)$ can be solved by

$$
\begin{aligned}
\hat{a}_j^{out}(\omega) =& m_1^j(\omega)\hat{b}^{in}(\omega) + m_2^j(\omega)\hat{b}^{in\dagger}(-\omega) + m_3^j(\omega)\hat{a}_A^{in}(\omega) \\
&+ m_4^j(\omega)\hat{a}_A^{in\dagger}(-\omega) + m_5^j(\omega)\hat{a}_B^{in}(\omega) + m_6^j(\omega)\hat{a}_B^{in\dagger}(-\omega)
\end{aligned}
\tag{19}
$$

where

$$
\begin{aligned}
m_1^A &= i\sqrt{\kappa_A\gamma_m}g_A u_2 v_2 w_1 w_2/z, \\
m_2^A &= i\sqrt{\kappa_A\gamma_m}g_A u_1 v_2 w_1 w_2/z, \\
m_3^A &= \kappa_A\big((u_1 - u_2)\big(g_B^2 v_2(w_1 - w_2) + g_A^2 w_1 w_2\big) + u_1 u_2 v_2 w_1 w_2\big)/z - 1, \\
m_4^A &= \kappa_A\big(g_A^2(u_1 - u_2)w_1 w_2\big)/z, \\
m_5^A &= \sqrt{\kappa_A\kappa_B}(g_A g_B(u_1 - u_2)v_2 w_2)/z, \\
m_6^A &= \sqrt{\kappa_A\kappa_B}(g_A g_B(u_1 - u_2)v_2 w_1)/z,
\end{aligned}
\tag{20}
$$

and

$$
\begin{aligned}
m_1^B &= i\sqrt{\kappa_B\gamma_m}g_B u_2 v_1 v_2 w_2/z, \\
m_2^B &= i\sqrt{\kappa_B\gamma_m}g_B u_1 v_1 v_2 w_2/z, \\
m_3^B &= \sqrt{\kappa_A\kappa_B}(g_A g_B(u_1 - u_2)v_2 w_2)/z, \\
m_4^B &= \sqrt{\kappa_A\kappa_B}(g_A g_B(u_1 - u_2)v_1 w_2)/z, \\
m_5^B &= \kappa_B\big((u_1 - u_2)\big(g_B^2 v_1 v_2 + g_A^2(v_1 - v_2)w_2\big) + u_1 u_2 v_1 v_2 w_2\big)/z - 1, \\
m_6^B &= \kappa_B\big(g_B^2(u_1 - u_2)v_1 v_2\big)/z,
\end{aligned}
\tag{21}
$$

with $z = (u_1 - u_2)\big(g_B^2 v_1 v_2(w_1 - w_2) + g_A^2(v_1 - v_2)w_1 w_2\big) + u_1 u_2 v_1 v_2 w_1 w_2$. Furthermore, by introducing two phase-quadrature operators

$$
X(\omega) = \frac{1}{2}\sum_{j=A,B}\Big[a_j^{out}(\omega) + a_j^{out\dagger}(-\omega)\Big],
\tag{22}
$$

and

$$
Y(\omega) = \frac{1}{2i}\sum_{j=A,B}\Big[a_j^{out}(\omega) - a_j^{out\dagger}(-\omega)\Big],
\tag{23}
$$

the squeezing spectra $S_{XX}(\omega)$ and $S_{YY}(\omega)$ can be calculated by $\langle X(\omega)X(\omega')\rangle = 2\pi S_{XX}(\omega)\delta(\omega + \omega')$ and $\langle Y(\omega)Y(\omega')\rangle = 2\pi S_{YY}(\omega)\delta(\omega + \omega')$ [43]. The output two-mode cavity field is squeezed if $S_2(\omega) = S_{XX}(\omega) + S_{YY}(\omega) < 1$.

In order to realize the two-mode squeezing light in steady state, two optical tweezers A and B are detuned to the red sideband (red-red), or the optical tweezers A is detuned to red sideband while the optical tweezers B is detuned to blue sideband (red-blue). In the red-blue case, the system will be stable in the blue sideband if the cavity photons are quickly lost to the vacuum. So, the cavity decay rates are assumed to $\kappa_B = 10\kappa_A = 3\omega_m$. As the torsional mode resonance in the blue sideband, the dynamics of the torsional motion

will be gradually amplified. In that case, the enhanced back-action interaction on the cavity mode will induce deeper squeezing. As shown in Figure 5, the squeezing of the red-blue case is much larger than that of the red-red case as the mechanical susceptibility of the levitated nano-ellipsoid responds in the resonant region.
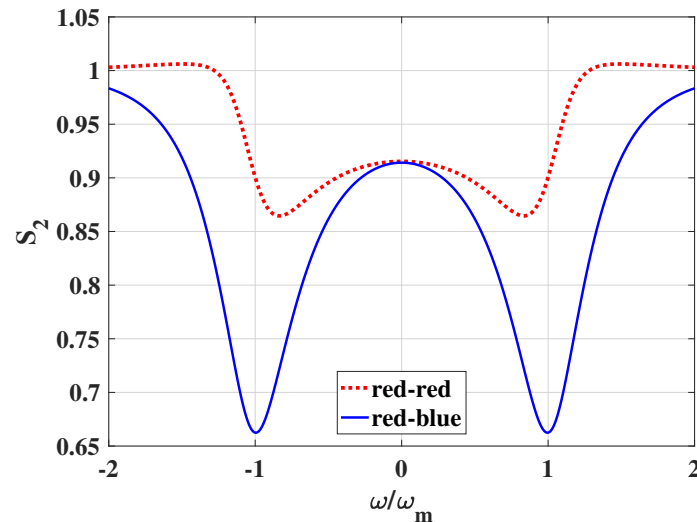

Figure 5. Squeezing spectrum of two output modes. The legend red-red represents both two optical tweezers in red sideband of the cavity mode. The legend red-blue denotes the optical tweezers A in red sideband while another tweezers B in blue sideband. The decay rates of the cavity mode are $\kappa_A = 0.3\omega_m$ and $\kappa_B = 3\omega_m$. Two tweezers are different in wavelength $\lambda_A = 780$ nm ($\lambda_B = 980$ nm). Other parameters are the same as Figure 3.

Next, we will analyze the two-mode squeezing from the view of system stability. As shown in Figure 6a, none of $S_2(\omega)$ is lower than 0.5 (3 dB). Obviously, there is a narrow and suddenly interrupted area, which splits the blue area into two parts. By comparing with Figure 6b, it corresponds to the critical boundary between the stable and unstable regions. The larger κ_B and smaller κ_A would make the system more stable. However, the squeezing will be reduced for the weak back-action. The maximum $S_2(\omega)$ reaches its maximum as the system approaches the dynamical instability [40].
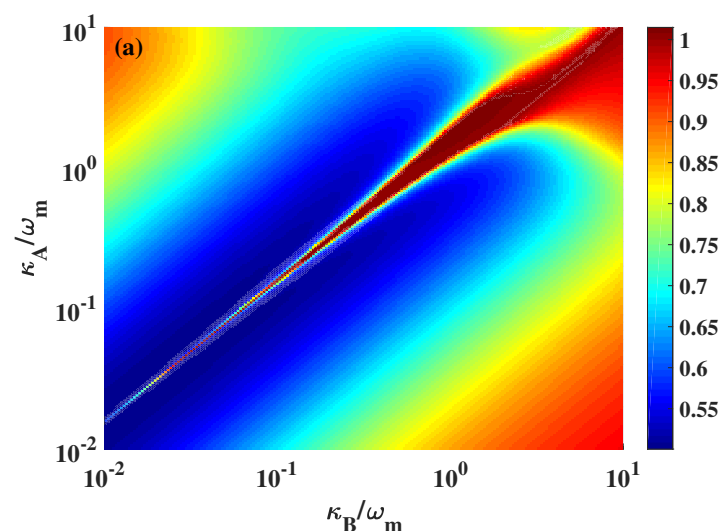

Figure 6. *Cont.*
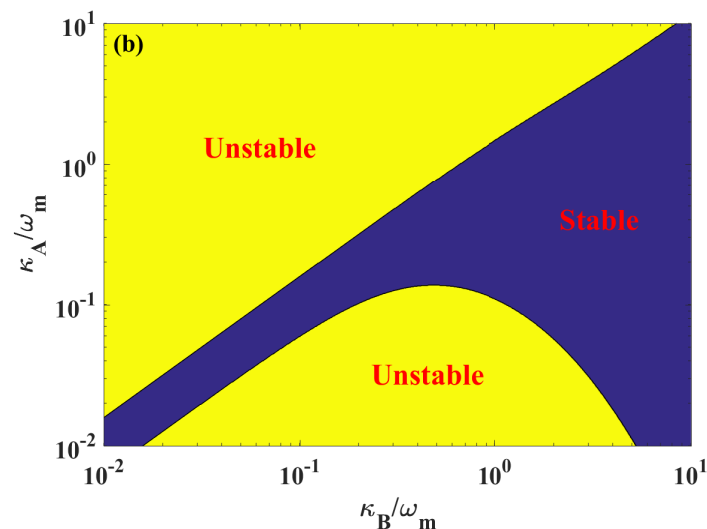
Figure 6. $S_2(\omega)$ (**a**) and the maximum eigenvalue of Equation (7) (**b**) as a function of the cavity decay rate κ_j. The detunings are set to the red and blue sideband $\Delta_A = -\Delta_B = \omega_m$, respectively. In picture (**b**), the yellow area means the maximum eigenvalue of Equation (7) is non-negative. According to the Routh–Hurwitz stability criterion [41], the system becomes instable in the long time limit. Conversely, the blue area denotes the system is stable. Other parameters are the same as Figure 5.

In Figure 7, we assume that the power of optical tweezer A is fixed at $P_A = 0.1$ W. Noted that the optical tweezer A is set to the red sideband of cavity mode, while optical tweezer B is detuned to the blue sideband. With the power P_B from 0.05 W to 0.15 W, $S_2(\omega)$ decreases at $\omega \approx \omega_m$ for the enhancement of the back-action interaction. As the power P_B up to 0.5 W, there is no squeezing on $\omega \approx \omega_m$. The amplified torsional motion is overlarge on resonance. It results in the instability of the system, which shows the destruction of squeezing.
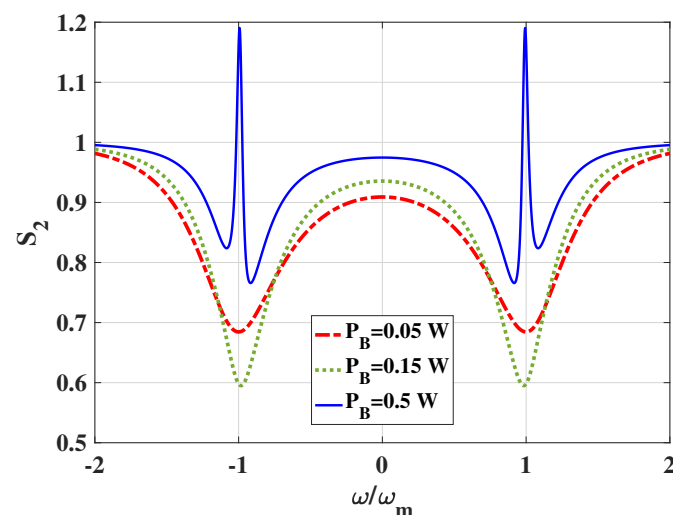

Figure 7. $S_2(\omega)$ as a function of P_B. The power of optical tweezer A in focus is set to $P_A = 0.1$ W. Tweezer A is detuned to the red sideband while tweezer B is set to be the blue sideband. Other parameters are the same as Figure 5.

5. Conclusions

We have proposed the squeezing light source based on an optically levitated nano-ellipsoid, which couples with a cavity. By the coherent scattering mechanism, the ultra-strong coupling between the cavity field and torsional mode of the nano-ellipsoid could be realized under the current experimental parameters. If the optical tweezers are on the red

sideband of the cavity mode, the single-mode squeezed light source (17 dB squeezing) can be realized even at room temperature. It is noteworthy that both the strong and broadband squeezing light can be achieved under the bad cavity condition. In order to achieve the two-mode squeezing light two optical tweezers are applied to trap the nano-particle at the same time. One is on the red sideband, while another is on the blue sideband. The two-mode squeezing of the lights is sensitive to the system stability, which depends on both the cavity decay rates and the power of the optical tweezers. When the system dynamics are close to the boundary of the stable regime, the two-mode squeezing can be maximized. However, two-mode squeezing can not be over the 3 dB limit in our current scheme. In future, the 3 dB limit can be overcome either by feedback [44] or by the reservoir-engineering method [45].

Author Contributions: Writing—original draft preparation, G.L. and Z.-Q.Y.; writing—review and editing, G.L. and Z.-Q.Y.; visualization, G.L. and Z.-Q.Y.; supervision, Z.-Q.Y.; project administration, Z.-Q.Y.; funding acquisition, Z.-Q.Y. All authors have read and agreed to the published version of the manuscript.

Institutional Review Board Statement: Not applicable.

Informed Consent Statement: Not applicable.

Data Availability Statement: Not applicable.

Conflicts of Interest: The authors declare no conflict of interest.

Appendix A. Polarization Tensor

An uniform isotropic non-dispersive ellipsoid is assumed to be smaller than the wave length of the tweezers λ_j. By this setting, the dipole approximation is performed. The corresponding polarizability of the nano-ellipsoid in a semiaxis k is [46]

$$\alpha_k = 4\pi abc\varepsilon_0 \frac{\varepsilon_r - \varepsilon_0}{3\varepsilon_0 + 3L_k(\varepsilon_r - \varepsilon_0)} \tag{A1}$$

where $k = \{a, b, c\}$ and $L_k = \frac{abc}{2}\int_0^\infty \frac{ds}{(s+j^2)(s+a^2)^{1/2}(s+b^2)^{1/2}(s+c^2)^{1/2}}$. With $a > b = c$, L_k can be analytically solved by

$$L_a = \frac{1-e^2}{e^2}\left(-1 + \frac{1}{2e}\ln\frac{1+e}{1-e}\right),$$

$$L_a + L_b + L_c = 1, \tag{A2}$$

$$L_b = L_c$$

where $e = \sqrt{1 - b^2/a^2}$ denotes the eccentricity. Then the polarizability tensor for the ellipsoid is given as the matrix product:

$$\hat{\alpha} = \hat{S}^{-1}\hat{\alpha}_0\hat{S}, \tag{A3}$$

where $\hat{\alpha}_0 = diag\{\alpha_a, \alpha_b, \alpha_c\}$ and $\hat{S} = \begin{vmatrix} \cos\theta & 0 & -\sin\theta \\ 0 & 1 & 0 \\ \sin\theta & 0 & \cos\theta \end{vmatrix}\begin{vmatrix} \cos\phi & \sin\phi & 0 \\ -\sin\phi & \cos\phi & 0 \\ 0 & 0 & 1 \end{vmatrix}$.

Appendix B. Hamiltonian for Coherent Scattering

As the size of the ellipsoid is assumed to be smaller than the wavelength of the optical tweezers, the dipole approximation is appropriate. The dipole moment is given as

$\hat{P} = \hat{\alpha}(\theta, \phi)\hat{E}(r, t)$, where $\alpha(\theta, \phi)$ is the polarization tensor characterized by the rotating angles θ and ϕ, $\hat{E}(r, t)$ is the electric field of the incoming beams. The Hamiltonian interaction between the nano-ellipsoid and electric field can be written as [24,47]

$$\hat{H}_I = -\frac{1}{2}\hat{\alpha}(\theta, \phi)\hat{E}^2(r, t) \tag{A4}$$

where

$$\hat{E}(r, t) = \sum_{j=A,B}\left(E_C^j(r) + \varepsilon_T^j(r, t)\right). \tag{A5}$$

$E_C^j(r) = \sqrt{\frac{\hbar\omega_c^j}{2\varepsilon_0 V_c^j}}\left[f^j(r)\hat{a}_j + H.c.\right]$ is the electric field in cavity mode and $\hat{\varepsilon}_T^j(r, t) = [E_T^j(r)e^{i\omega_j t} + c.c.]/2$ is the tweezers field with Gaussian form $E_T^j(r) = E_0^j\frac{w_{t0}^j}{w_t^j(z)}e^{-\frac{x^2+y^2}{w_t^j(z)w_t^j(z)}}e^{i\omega_j t}e^{ik_t^j z}e^{i\psi_t^j(r)}$. $\hat{a}_j$ and $\hat{a}_j^\dagger$ are the bosonic annihilation and creator operators of cavity mode. ω_j (ω_c^j), k_t^j (k_c^j), and w_{t0}^j (w_c^j) are the frequency, wave number, and beam waist of the optical tweezers (cavity modes). $V_c^j = \pi d w_c^j w_c^j/4$ denotes the cavity volume where d is the cavity length. The mode function $f^j(y)$ depends on the boundary of the cavity, which can be written as $f^j(r) = cos(k_c^j y + \psi_j)$ in y axis. $E_0^j = \sqrt{4P_j/\pi\varepsilon_0 c w_{t0}^j}$ and $w_t^j(z) = w_{t0}^j\sqrt{1 + z^2/z_R^{j2}}$ are the amplitude and beam waist of the tweezers. $z_R^j = \pi w_{t0}^j w_{t0}^j/\lambda_j$ and $\psi_t^j(r)$ are the Rayleigh range and Gouy phase of the tweezers. P_j, c, and λ_j are the power, speed, and wavelength of the tweezers.

By inserting Equation (A5) to Equation (A4), the Hamiltonian can be written as $H_I = H_{T-T} + H_{C-C} + H_{T-C}$ where

$$H_{T-T} = -\frac{1}{2}\hat{\alpha}(\theta, \phi)\sum_{j=A,B}\varepsilon_T^j(r, t)\varepsilon_T^j(r, t), \tag{A6}$$

$$H_{C-C} = -\frac{1}{2}\hat{\alpha}(\theta, \phi)\sum_{j=A,B}E_C^j(r)E_C^j(r), \tag{A7}$$

and

$$H_{T-C} = -\hat{\alpha}(\theta, \phi)\sum_{j=A,B}\varepsilon_T^j(r, t)E_C^j(r). \tag{A8}$$

Then, we assume that the nano-ellipsoid is fixed at the origin ($r = 0$), and only the torsional motion on θ and ϕ is under considered. That is, when $\theta(\phi) \to 0$, one can expand the H_{T-T} to the second order of $\theta(\phi)$. The torsional frequency of the nano-ellipsoid is

$$\omega_{\theta(\phi)} = \sqrt{\left(E_0^A E_0^A + E_0^B E_0^B\right)(\alpha_a - \alpha_b)\Big/2I} \tag{A9}$$

where $I = M(a^2 + b^2)/5$ denotes the inertia of the ellipsoid. M is the mass of the nano-ellipsoid. The corresponding intrinsic optomechanical coupling and coherent scattering coupling can be derived by expanding the H_{C-C} and H_{C-T} to the first order of $\theta(\phi)$ as $\theta \to \pi/4, \phi = 0(\phi \to \pi/4, \theta = 0)$, given as

$$g_{\theta(\phi)}^j = \frac{(\alpha_a - \alpha_b)\omega_c^j\xi_0^{\theta(\phi)}\cos^2(\varphi_j)}{2\varepsilon_0 V_c^j}, \tag{A10}$$

$$g_{s\theta(s\phi)}^j = (\alpha_a - \alpha_b)E_0\xi_0^{\theta(\phi)}\cos(\varphi_j)\sqrt{\frac{\omega_c^j}{8\hbar\varepsilon_0 V_c^j}} \tag{A11}$$

where $\xi_0^{\theta(\phi)} = \sqrt{\hbar/2I\omega_{\theta(\phi)}}$ is the zero-point fluctuation of torsion mode. It is noted that the torsion motion can be decoupled from the center-of-mass motion by moving the optical tweezers to the anti-node of the cavity mode ($\varphi_j = 0$) [37]. Moreover, because $g^j_{\theta(\phi)}$ is much smaller than the $g^j_{s\theta(s\phi)}$, the coherent scattering coupling $g^j_{s\theta(s\phi)}$ is under considered. Then the Hamiltonian for the interaction picture can be read by [24]

$$\hat{H} = \hbar\Delta_j \hat{a}_j^\dagger \hat{a}_j + \hbar\omega_m \hat{b}^\dagger \hat{b} - \hbar \sum_{j=A,B} g_j \left(\hat{a}_j^\dagger + \hat{a}_j \right) \left(\hat{b}^\dagger + \hat{b} \right) \tag{A12}$$

where $\Delta_j = \omega_c^j - \omega_j$, ω_m denotes the torsional frequency $\omega_{\theta(\phi)}$, and g_j represents the coherent scattering coupling $g^j_{s\theta(s\phi)}$. In this Hamiltonian, the first two terms denote the free Hamiltonian for the cavity modes and torsional mode, while the last term describes the coherent scattering interactions between the cavity modes and torsional mode.

Appendix C. Damping for Torsional Motion

As the nano-ellipsoid optically trapped in a high vacuum environment, the collision of surrounding gas on nano-ellipsoid leads to the change of angular momentum. The damping rate for the torsional motion is given by [48]

$$\gamma_\phi = \frac{5\rho_a \bar{v} a^3 \sqrt{1-e^2}}{8\rho(a^2+b^2)} \left[\gamma_{ac} \left(f_1 + \left(1-e^2\right) f_2 \right) + 3 \left(1 - \gamma_{ac} \frac{6-\pi}{8} \right) e^4 f_3 \right] \tag{A13}$$

where

$$f_1 = \frac{3}{8e^2} \left[\frac{1}{e} \arcsin(e) - \left(1-2e^2\right)\sqrt{1-e^2} \right],$$

$$f_2 = \frac{3}{16e^2} \left[\left(1+2e^2\right)\sqrt{1-e^2} - \frac{1}{e}\arcsin(e)\left(1-4e^2\right) \right], \tag{A14}$$

$$f_3 = \frac{1}{4e^4} \left[\left(3-2e^2\right)\sqrt{1-e^2} + \frac{1}{e}\arcsin(e)\left(4e^2-3\right) \right].$$

$\rho_a = m_a p / k_B T_a$ is the mass density, where m_a, p, and T_a are atom mass, pressure, and temperature of the residual gas. $\bar{v} = \sqrt{8k_B T_a / \pi m_a}$ is the mean thermal velocity and ρ is the density of the nano-ellipsoid. γ_{ac} denotes the accommodation efficient which charges the diffuse and specular reflection of ellipsoidal surface.

References

1. Aasi, J.; Abadie, J.; Abbott, B.P.; Abbott, R.; Abbott, T.D.; Abernathy, M.R.; Adams, C.; Adams, T.; Addesso, P.; Adhikari, R.X.; et al. Enhanced sensitivity of the LIGO gravitational wave detector by using squeezed states of light. *Nat. Photonics* **2013**, *7*, 613–619, doi:10.1038/nphoton.2013.177.
2. Clark, J.B.; Lecocq, F.; Simmonds, R.W.; Aumentado, J.; Teufel, J.D. Sideband cooling beyond the quantum backaction limit with squeezed light. *Nature* **2017**, *541*, 191–195, doi:10.1038/nature20604.
3. Zeytinoğlu, S.; İmamoğlu, A.; Huber, S. Engineering matter interactions using squeezed vacuum. *Phys. Rev. X* **2017**, *7*, 021041, doi:10.1103/PhysRevX.7.021041.
4. Peano, V.; Houde, M.; Brendel, C.; Marquardt, F.; Clerk, A.A. Topological phase transitions and chiral inelastic transport induced by the squeezing of light. *Nat. Commun.* **2016**, *7*, 10779, doi:10.1038/ncomms10779.
5. Fabre, C.; Pinard, M.; Bourzeix, S.; Heidmann, A.; Giacobino, E.; Reynaud, S. Quantum-noise reduction using a cavity with a movable mirror. *Phys. Rev. A* **1994**, *49*, 1337–1343, doi:10.1103/PhysRevA.49.1337.
6. Mancini, S.; Tombesi, P. Quantum noise reduction by radiation pressure. *Phys. Rev. A* **1994**, *49*, 4055–4065, doi:10.1103/PhysRevA.49.4055.
7. Wu, L.A.; Kimble, H.; Hall, J.; Wu, H. Generation of squeezed states by parametric down conversion. *Phys. Rev. Lett.* **1986**, *57*, 2520, doi:10.1103/PhysRevLett.57.2520.
8. Aspelmeyer, M.; Kippenberg, T.J.; Marquardt, F. Cavity optomechanics. *Rev. Mod. Phys.* **2014**, *86*, 1391, doi:10.1103/RevModPhys.86.1391.
9. Purdy, T.P.; Yu, P.L.; Peterson, R.W.; Kampel, N.S.; Regal, C.A. Strong Optomechanical Squeezing of Light. *Phys. Rev. X* **2013**, *3*, 031012, doi:10.1103/PhysRevX.3.031012.

10. Ockeloen-Korppi, C.; Damskägg, E.; Pirkkalainen, J.M.; Heikkilä, T.; Massel, F.; Sillanpää, M. Noiseless quantum measurement and squeezing of microwave fields utilizing mechanical vibrations. *Phys. Rev. Lett.* **2017**, *118*, 103601, doi:10.1103/PhysRevLett.118.103601.

11. Pontin, A.; Biancofiore, C.; Serra, E.; Borrielli, A.; Cataliotti, F.; Marino, F.; Prodi, G.; Bonaldi, M.; Marin, F.; Vitali, D. Frequency-noise cancellation in optomechanical systems for ponderomotive squeezing. *Phys. Rev. A* **2014**, *89*, 033810, doi:10.1103/PhysRevA.89.033810.

12. Yin, Z.q.; Han, Y.J. Generating EPR beams in a cavity optomechanical system. *Phys. Rev. A* **2009**, *79*, 024301, doi:10.1103/PhysRevA.79.024301.

13. Sainadh, S.; Kumar, M.A. Effects of linear and quadratic dispersive couplings on optical squeezing in an optomechanical system. *Phys. Rev. A* **2015**, *92*, 033824, doi:10.1103/PhysRevA.92.033824.

14. Zippilli, S.; Di Giuseppe, G.; Vitali, D. Entanglement and squeezing of continuous-wave stationary light. *New J. Phys.* **2015**, *17*, 043025, doi:10.1088/1367-2630/17/4/043025.

15. Kronwald, A.; Marquardt, F.; Clerk, A.A. Dissipative optomechanical squeezing of light. *New J. Phys.* **2014**, *16*, 063058, doi:10.1088/1367-2630/16/6/063058.

16. Yin, Z.q.; Li, T.; Zhang, X.; Duan, L. Large quantum superpositions of a levitated nanodiamond through spin-optomechanical coupling. *Phys. Rev. A* **2013**, *88*, 033614, doi:10.1103/PhysRevA.88.033614.

17. Romero-Isart, O.; Pflanzer, A.C.; Blaser, F.; Kaltenbaek, R.; Kiesel, N.; Aspelmeyer, M.; Cirac, J.I. Large quantum superpositions and interference of massive nanometer-sized objects. *Phys. Rev. Lett.* **2011**, *107*, 020405, doi:10.1103/PhysRevLett.107.020405.

18. Chen, X.Y.; Yin, Z.Q. High-precision gravimeter based on a nano-mechanical resonator hybrid with an electron spin. *Opt. Express* **2018**, *26*, 31577, doi:10.1364/OE.26.031577.

19. Huang, Y.; Guo, Q.; Xiong, A.; Li, T.; Yin, Z.q. Classical and quantum time crystals in a levitated nanoparticle without drive. *Phys. Rev. A* **2020**, *102*, 023113, doi:10.1103/PhysRevA.102.023113.

20. Huang, Y.; Li, T.; Yin, Z.q. Symmetry-breaking dynamics of the finite-size Lipkin-Meshkov-Glick model near ground state. *Phys. Rev. A* **2018**, *97*, 012115, doi:10.1103/PhysRevA.97.012115.

21. Zhang, H.; Chen, X.; Yin, Z.q. Quantum Information Processing and Precision Measurement Using a Levitated Nanodiamond. *Adv. Quantum Technol.* **2021**, *4*, 2000154, doi:10.1002/qute.202000154.

22. Chang, D.E.; Regal, C.; Papp, S.; Wilson, D.; Ye, J.; Painter, O.; Kimble, H.J.; Zoller, P. Cavity opto-mechanics using an optically levitated nanosphere. *Proc. Natl. Acad. Sci. USA* **2010**, *107*, 1005–1010, doi:10.1073/pnas.0912969107.

23. Rashid, M.; Tufarelli, T.; Bateman, J.; Vovrosh, J.; Hempston, D.; Kim, M.; Ulbricht, H. Experimental realization of a thermal squeezed state of levitated optomechanics. *Phys. Rev. Lett.* **2016**, *117*, 273601, doi:10.1103/PhysRevLett.117.273601.

24. Gonzalez-Ballestero, C.; Maurer, P.; Windey, D.; Novotny, L.; Reimann, R.; Romero-Isart, O. Theory for cavity cooling of levitated nanoparticles via coherent scattering: Master equation approach. *Phys. Rev. A* **2019**, *100*, 013805, doi:10.1103/PhysRevA.100.013805.

25. Toroš, M.; Delić, U.; Hales, F.; Monteiro, T.S. Coherent-scattering two-dimensional cooling in levitated cavity optomechanics. *Phys. Rev. Res.* **2021**, *3*, 023071, doi:10.1103/PhysRevResearch.3.023071.

26. Delić, U.; Reisenbauer, M.; Dare, K.; Grass, D.; Vuletić, V.; Kiesel, N.; Aspelmeyer, M. Cooling of a levitated nanoparticle to the motional quantum ground state. *Science* **2020**, *367*, 892–895, doi:10.1126/science.aba3993.

27. Schäfer, J.; Rudolph, H.; Hornberger, K.; Stickler, B.A. Cooling nanorotors by elliptic coherent scattering. *Phys. Rev. Lett.* **2021**, *126*, 163603, doi:10.1103/PhysRevLett.126.163603.

28. Magrini, L.; Rosenzweig, P.; Bach, C.; Deutschmann-Olek, A.; Hofer, S.G.; Hong, S.; Kiesel, N.; Kugi, A.; Aspelmeyer, M. Real-time optimal quantum control of mechanical motion at room temperature. *Nature* **2021**, *595*, 373–377, doi:10.1038/s41586-021-03602-3.

29. Tebbenjohanns, F.; Mattana, M.L.; Rossi, M.; Frimmer, M.; Novotny, L. Quantum control of a nanoparticle optically levitated in cryogenic free space. *Nature* **2021**, *595*, 378–372, doi:10.1038/s41586-021-03617-w.

30. de los Ríos Sommer, A.; Meyer, N.; Quidant, R. Strong optomechanical coupling at room temperature by coherent scattering. *Nat. Commun.* **2021**, *12*, 276–281, doi:10.1038/s41467-020-20419-2.

31. Asenbaum, P.; Kuhn, S.; Nimmrichter, S.; Sezer, U.; Arndt, M. Cavity cooling of free silicon nanoparticles in high vacuum. *Nat. Commun.* **2013**, *4*, 1–7, doi:10.1038/ncomms3743.

32. Millen, J.; Monteiro, T.S.; Pettit, R.; Vamivakas, A.N. Optomechanics with levitated particles. *Rep. Prog. Phys.* **2020**, *83*, 026401, doi:10.1088/1361-6633/ab6100.

33. Jain, V.; Gieseler, J.; Moritz, C.; Dellago, C.; Quidant, R.; Novotny, L. Direct measurement of photon recoil from a levitated nanoparticle. *Phys. Rev. Lett.* **2016**, *116*, 243601, doi:10.1103/PhysRevLett.116.243601.

34. Černotík, O.; Filip, R. Strong mechanical squeezing for a levitated particle by coherent scattering. *Phys. Rev. Res.* **2020**, *2*, 013052, doi:10.1103/PhysRevResearch.2.013052.

35. Yin, Z.Q.; Geraci, A.A.; Li, T. Optomechanics of levitated dielectric particles. *Int. J. Mod. Phys. B* **2013**, *27*, 1330018, doi:10.1142/S0217979213300181.

36. Kockum, A.F.; Miranowicz, A.; De Liberato, S.; Savasta, S.; Nori, F. Ultrastrong coupling between light and matter. *Nat. Rev. Phys.* **2019**, *1*, 19–40, doi:10.1038/s42254-018-0006-2.

37. Li, G.; Yin, Z.q. Steady motional entanglement between two distant levitated nanoparticles. *arXiv* **2021**, arXiv:2111.11620.

38. Hoang, T.M.; Ma, Y.; Ahn, J.; Bang, J.; Robicheaux, F.; Yin, Z.Q.; Li, T. Torsional optomechanics of a levitated nonspherical nanoparticle. *Phys. Rev. Lett.* **2016**, *117*, 123604, doi:10.1103/PhysRevLett.117.123604.

39. Ahn, J.; Xu, Z.; Bang, J.; Deng, Y.H.; Hoang, T.M.; Han, Q.; Ma, R.M.; Li, T. Optically levitated nanodumbbell torsion balance and GHz nanomechanical rotor. *Phys. Rev. Lett.* **2018**, *121*, 033603, doi:10.1103/PhysRevLett.121.033603.

40. Genes, C.; Mari, A.; Tombesi, P.; Vitali, D. Robust entanglement of a micromechanical resonator with output optical fields. *Phys. Rev. A* **2008**, *78*, 032316, doi:10.1103/PhysRevA.78.032316.

41. Vitali, D.; Gigan, S.; Ferreira, A.; Böhm, H.; Tombesi, P.; Guerreiro, A.; Vedral, V.; Zeilinger, A.; Aspelmeyer, M. Optomechanical entanglement between a movable mirror and a cavity field. *Phys. Rev. Lett.* **2007**, *98*, 030405, doi:10.1103/PhysRevLett.98.030405.

42. Zhang, Z.C.; Wang, Y.P.; Yu, Y.F.; Zhang, Z.M. Quantum squeezing in a modulated optomechanical system. *Opt. Express* **2018**, *26*, 11915–11927, doi:10.1364/OE.26.011915.

43. Li, Z.; Ma, S.l.; Li, F.l. Generation of broadband two-mode squeezed light in cascaded double-cavity optomechanical systems. *Phys. Rev. A* **2015**, *92*, 023856, doi:10.1103/PhysRevA.92.023856.

44. Vinante, A.; Falferi, P. Feedback-enhanced parametric squeezing of mechanical motion. *Phys. Rev. Lett.* **2013**, *111*, 207203, doi:10.1103/PhysRevLett.111.207203.

45. Dassonneville, R.; Assouly, R.; Peronnin, T.; Clerk, A.; Bienfait, A.; Huard, B. Dissipative stabilization of squeezing beyond 3 dB in a microwave mode. *PRX Quantum* **2021**, *2*, 020323, doi:10.1103/PRXQuantum.2.020323.

46. Bohren, C.F.; Huffman, D.R. *Absorption and Scattering of Light by Small Particles*; John Wiley & Sons: Hoboken, NJ, USA, 1983.

47. Gonzalez-Ballestero, C.; Aspelmeyer, M.; Novotny, L.; Quidant, R.; Romero-Isart, O. Levitodynamics: Levitation and control of microscopic objects in vacuum. *Science* **2021**, *374*, eabg3027, doi:10.1126/science.abg3027.

48. Halbritter, J. Torque on a rotating ellipsoid in a rarefied gas. *Z. Für Naturforsch. A* **1974**, *29*, 1717–1722, doi:10.1515/zna-1974-1203.